Topotecan Central Nervous System Penetration Is Altered by a Tyrosine Kinase Inhibitor

Yanli Zhuang,[1] Charles H. Fraga,[1] K. Elaine Hubbard,[1] Nikolaus Hagedorn,[1] John C. Panetta,[1] Christopher M. Waters,[2] and Clinton F. Stewart[1]

[1]Department of Pharmaceutical Sciences, St. Jude Children's Research Hospital and [2]Department of Physiology, College of Medicine, University of Tennessee Health Science Center, Memphis, Tennessee

Abstract

A potential strategy to increase the efficacy of topotecan to treat central nervous system (CNS) malignancies is modulation of the activity of ATP-binding cassette (ABC) transporters at the blood-brain and blood-cerebrospinal fluid barriers to enhance topotecan CNS penetration. This study focused on topotecan penetration into the brain extracellular fluid (ECF) and ventricular cerebrospinal fluid (CSF) in a mouse model and the effect of modulation of ABC transporters at the blood-brain and blood-cerebrospinal fluid barriers by a tyrosine kinase inhibitor (gefitinib). After 4 and 8 mg/kg topotecan i.v., the brain ECF to plasma AUC ratio of unbound topotecan lactone was 0.21 ± 0.04 and 0.61 ± 0.16, respectively; the ventricular CSF to plasma AUC ratio was 1.18 ± 0.10 and 1.30 ± 0.13, respectively. To study the effect of gefitinib on topotecan CNS penetration, 200 mg/kg gefitinib was administered orally 1 hour before 4 mg/kg topotecan i.v. The brain ECF to plasma AUC ratio of unbound topotecan lactone increased by 1.6-fold to 0.35 ± 0.04, which was significantly different from the ratio without gefitinib ($P < 0.05$). The ventricular CSF to plasma AUC ratio significantly decreased to 0.98 ± 0.05 ($P < 0.05$). Breast cancer resistance protein 1 (Bcrp1), an efficient topotecan transporter, was detected at the apical aspect of the choroid plexus in FVB mice. In conclusion, topotecan brain ECF penetration was lower compared with ventricular CSF penetration. Gefitinib increased topotecan brain ECF penetration but decreased the ventricular CSF penetration. These results are consistent with the possibility that expression of Bcrp1 and P-glycoprotein at the apical side of the choroid plexus facilitates an influx transport mechanism across the blood-cerebrospinal fluid barrier, resulting in high topotecan CSF penetration. (Cancer Res 2006; 66(23): 11305-13)

Introduction

Topotecan [(*S*)-9-dimethylaminomethyl-10-hydroxyamptothecin hydrochloride] is a semisynthetic water-soluble camptothecin analogue that specifically targets topoisomerase I (1, 2). In preclinical studies, topotecan showed antitumor activity against pediatric xenograft models of primary central nervous system (CNS) tumors, such as medulloblastoma and high-grade gliomas (3, 4). Results of recent clinical trials with topotecan have shown promising antitumor activity in children with high-risk medulloblastoma (5); however, the results of clinical trials of topotecan for gliomas have been disappointing (6–8).

In general, the poor response of primary CNS tumors to chemotherapy drugs is multifactorial, but inadequate delivery of active compounds to the tumor site in the brain is certainly a well-known mechanism (9, 10). For systemically administered drugs to enter the brain, they must pass across either of two membrane barrier systems, the blood-brain barrier or the blood-cerebrospinal fluid barrier. The blood-brain barrier regulates drug distribution into the brain extracellular fluid (ECF), whereas the blood-cerebrospinal fluid barrier regulates drug distribution into cerebrospinal fluid (CSF). It is important to distinguish distribution of drugs into brain ECF or CSF to provide insight into the potential efficacy of a drug for specific CNS tumors, such as tissue-based (e.g., gliomas) or CSF-related (e.g., medulloblastoma) tumors. Due to the anatomic and physiologic differences between the blood-brain and blood-cerebrospinal fluid barriers, distribution of anticancer drugs into brain ECF and CSF may differ (11).

The presence of ATP-binding cassette (ABC) proteins is one physiologic difference between the blood-brain and blood-cerebrospinal fluid barriers that may alter drug penetration. Many of these transporters function as efflux pumps at the blood-brain and blood-cerebrospinal fluid barriers to reduce drug penetration into the brain. Moreover, these proteins are well known to account for multidrug resistance in primary CNS malignancies (9). Numerous studies have shown that topotecan is a substrate for P-glycoprotein (P-gp; ABCB1; refs. 12, 13), MRP4 (ABCC4; ref. 14), and breast cancer resistance protein (BCRP; ABCG2; refs. 15, 16). After oral coadministration of topotecan and elacridar, a potent inhibitor for BCRP and P-gp (both of which are highly expressed in the intestines), the apparent oral bioavailability of topotecan was increased from 40% to 97% (17). Thus, we hypothesized that modulation of ABC transporters at the blood-brain and blood-cerebrospinal fluid barriers might alter topotecan CNS penetration.

Many compounds have been shown to modulate ABC transporters, and recently our group has shown that the epidermal growth factor receptor (EGFR) tyrosine kinase inhibitors modulate the activity of multiple transporters (18). The 4-anilinoquinazolines are a group of compounds that inhibit the intracellular phosphorylation of numerous tyrosine kinases associated with transmembrane cell-surface receptors such as EGFR. The combination of EGFR tyrosine kinase inhibitors with cytotoxic agents enhances cytotoxicity *in vitro* and in mouse models, and the interaction of EGFR tyrosine kinase inhibitors with ABC transporters (e.g., BCRP, P-gp) has been suggested as a mechanism to explain this enhanced cytotoxicity (19–22). On the basis of *in vitro* results and the distribution of Bcrp1 in mouse tissues, we assessed the ability of a model tyrosine kinase inhibitor, gefitinib, to modulate the

Requests for reprints: Clinton F. Stewart, Department of Pharmaceutical Sciences, St. Jude Children's Research Hospital, 332 North Lauderdale Street, Memphis, TN 38105. Phone: 901-495-3365; Fax: 901-525-6869; E-mail: clinton.stewart@stjude.org.

doi:10.1158/0008-5472.CAN-06-0929

pharmacokinetics of the camptothecin analogue, irinotecan (23). Oral gefitinib coadministration dramatically increased the oral bioavailability of irinotecan (23). Gefitinib also increased topotecan oral absorption and decreased systemic clearance of topotecan. Pharmacokinetic studies in *Abcg2*$^{-/-}$ and *Mdr1a/1b*$^{-/-}$ mice showed that gefitinib inhibited both Bcrp1 and P-gp at clinically relevant concentrations (18). These data provided the conceptual framework for the present study examining the effect of the tyrosine kinase inhibitor gefitinib on the brain penetration of topotecan. The objectives of the present study were to determine the brain ECF and ventricular CSF penetration of topotecan in mice and to assess the effect of a tyrosine kinase inhibitor (i.e., gefitinib) on the brain parenchymal ECF and ventricular CSF penetration of topotecan.

Materials and Methods

Chemicals and drugs. Topotecan solutions for chromatography (1 mg/mL) were prepared in DMSO. For pharmacokinetic studies, topotecan hydrochloride (Hycamtin, GlaxoSmithKline, Philadelphia, PA) was prepared in sterile water for injection (1.0 or 2.0 mg/mL). Gefitinib tablets (Iressa, AstraZeneca), containing 250 mg gefitinib per tablet, were weighed and pulverized. Gefitinib powder was wet with 0.5% Tween 20 (20% v/v final volume) and suspended in carboxymethylcellulose (0.25% w/v) to final concentrations of 20 or 40 mg/mL. Acetonitrile and triethylamine were of high-performance liquid chromatography (HPLC) grade. All other chemicals and solvents used were of analytic grade or better.

Topotecan plasma protein binding. Topotecan lactone protein binding was studied in pooled murine plasma (Hilltop Lab Animals, Inc., Scottdale, PA), plasma from C57/B6-129 mice, and plasma from FVB mice. Topotecan was added to plasma aliquots from each source to make final topotecan lactone concentrations of 50, 500, and 5000 ng/mL. Spiked plasma (0.5 mL) was added to a Centrifree YM-30 (Millipore Corporation, Billerica, MA) sample reservoir and centrifuged at 2,000 × *g* for 20 minutes. Topotecan was extracted from the protein and ultrafiltrate portion of the device, respectively, by adding 50 μL of sample immediately to 200 μL of ice-cold methanol. Samples were analyzed by an HPLC method as previously reported (24, 25). Topotecan lactone fraction unbound was calculated as amount of unbound topotecan lactone divided by total amount of topotecan lactone in plasma.

Gefitinib plasma pharmacokinetics. Gefitinib was administered to female FVB mice (The Jackson Laboratory, Bar Harbor, ME) by oral gavage as a single dose of 100 or 200 mg/kg. The blood sampling strategy was designed based on a population pharmacokinetic approach with fixed sample size. Each mouse was randomly sampled three times out of seven sampling time points (0.25, 1, 2, 3, 6, 8, and 12 hours) by either retro-orbital bleed or by cardiac puncture at the final time point. At least four different animals contributed to each time point. Plasma gefitinib concentrations were measured using a previously described liquid-liquid extraction, liquid chromatography tandem mass spectrometry method (26). Briefly, samples were extracted with *tert*-butyl ether containing internal standard, separated on Phenomenex Synergy 4-μm MAX-RP C12 column (75 × 2.0 mm) with an isocratic mobile phase of acetonitrile/1.0% formic acid (30:70, v/v), and detected with a PE Sciex API 365 triple quadrupole MS using turbo ion spray source with positive ionization.

Topotecan plasma pharmacokinetics with and without gefitinib. For the topotecan population pharmacokinetic studies, six to eight female FVB mice (The Jackson Laboratory) per group were pretreated with either control vehicle or 200 mg/kg gefitinib orally 1 hour before the tail vein injection of topotecan (4 or 8 mg/kg). The blood sampling scheme was designed based on a population pharmacokinetic approach with a fixed sample size to minimize the blood volume removed from the animal. Each mouse was randomly sampled four times out of five sampling time points (0.25, 1, 2, 3, and 6 hours) by either retro-orbital bleed or by cardiac puncture at the final time point. At least four different animals contributed to each time point. For the topotecan pharmacokinetic studies in individual mice during microdialysis, plasma was obtained and 20-μL aliquots were added to 80 μL cold methanol (−30°C). Samples were vortex mixed vigorously and centrifuged at 10,000 rpm for 2 minutes. The supernatant was analyzed using an HPLC assay with fluorescence detection to determine topotecan lactone plasma concentrations as previously described (24, 25).

Animal preparation and brain surgery. To eliminate the possibility that gender-specific expression of genes would potentially confound topotecan pharmacokinetics and CNS penetration, we chose to use only female FVB mice (The Jackson Laboratory). These mice, which weighed 20 to 25 g, were maintained on a 12-hour light/dark cycles and were given free access to food and water. Brain surgery for the implantation of the microdialysis guide cannula was done as previously reported (27). Briefly, the mouse was anesthetized with ketamine (Abbott Laboratories, Chicago IL)/xylazine (Butler Company, Columbus, OH). A guide cannula with stylet (MD-2255, Bioanalytical Systems, West Lafayette, IN) was inserted in either the lateral ventricle (0.1 mm posterior to bregma suture, 2.0 mm lateral to sagittal suture, 2.0 mm ventral) or in the parenchyma (0.6 mm anterior to bregma suture, 2.0 mm lateral to sagittal suture, 2.0 mm ventral). Mice recovered for 3 to 5 days before the microdialysis experiment. All animal studies were conducted using protocols and conditions approved by the St. Jude Children's Research Hospital Institutional Animal Care and Use Committee.

Microdialysis in ventricular CSF and brain ECF. On the day of a microdialysis experiment, a probe with 1-mm active membrane (MBR-1-5 brain probe, Bioanalytical Systems) was primed and flushed with blank artificial CSF (NaCl 148 mmol/L, KCl 4 mmol/L, $MgCl_2$ 0.8 mmol/L, $CaCl_2$ 1.4 mmol/L, Na_2HPO_4 1.2 mmol/L, NaH_2PO_4 0.3 mmol/L, and dextrose 5 mmol/L, pH adjusted to 7.4; ref. 27). The stylet in the guide cannula was then replaced by the newly primed probe, which was allowed to equilibrate for ~1 hour after insertion. The perfusion rate of the syringe pump was set at 0.5 μL/min. Topotecan brain ECF or ventricular CSF distribution was evaluated in three to four mice per group at two dosage levels of 4 and 8 mg/kg. The effect of gefitinib on topotecan distribution into brain ECF or ventricular CSF was studied by pretreating the animal with gefitinib 1 hour before topotecan. Microdialysis samples were collected every 18 minutes and directly injected onto the microbore column without further processing (27). Topotecan carboxylate and lactone in dialysate were separated on a microbore reverse-phase chromatography column (0.8 × 150 mm) packed with C_{18}, 3-mm Inertsil particles (Dionex, Sunnyvale, CA), and detected with a fluorescence detector (emission, 370 nm; excitation, 520 nm). The mobile phase consisted of acetonitrile-triethylamine acetate buffer pH 4.5 (20:80, v/v) and the flow rate was 32 μL/min. Automatic injections were programmed through signaling from the HPLC pump (27).

During the microdialysis period, plasma samples were obtained from the mouse at 0.25, 1, and 3 hours after topotecan administration by retro-orbital bleed. The sampling times were chosen based on the limited sampling model developed using topotecan population pharmacokinetic variables as the priors. The plasma samples were processed and analyzed for topotecan lactone (24, 25). After the microdialysis experiment, the animal was euthanized and the brain was fixed in 10% neutral buffered formalin for 24 hours and embedded in paraffin. H&E-stained sections (4 μm) were examined microscopically to verify the location of the microdialysis probe track. If the intended purpose of the microdialysis study was to assess the topotecan ventricular CSF penetration and the probe was noted as outside the lateral ventricle on this microscopic examination, then the results from that study were excluded from analysis.

Microdialysis probe recovery. Because *in vivo* probe recovery may be significantly different from *in vitro* recovery, we investigated *in vivo* recovery of topotecan in each animal using the retrodialysis method with or without gefitinib treatment (28, 29). *In vitro* recovery studies done in our lab showed that topotecan lactone and carboxylate have the same recovery;[3] therefore, we used recovery of total topotecan to represent the recovery

[3] Unpublished data.

for each form of topotecan. A topotecan solution was prepared in artificial CSF and the total topotecan concentration (C_{in}) was determined by HPLC. The solution was perfused through the microdialysis probe and the total topotecan concentration (C_{out}) in the solution exiting the probe was measured. The recovery ($R_{topotecan}$) was estimated as shown in Eq. A.

$$R_{\text{topotecan}} = (C_{\text{in}} - C_{\text{out}})/C_{\text{in}} \quad \text{(A)}$$

Analysis of plasma pharmacokinetic data. Nonlinear mixed-effects modeling (NONMEM version V; ref. 30) was used to estimate the gefitinib population pharmacokinetic variables. Specifically, a one-compartment model with oral absorption was used to fit the gefitinib data. Apparent clearance (CL/*f*), apparent volume (*V*/*f*), and oral absorption (k_a) were estimated along with their SE estimates and the interindividual variability.

The goal of the plasma pharmacokinetic studies was to conduct them in the same mouse in which the microdialysis study was done; however, due to logistical limitations (e.g., blood volume), we were limited to no more than three plasma samples per study. Thus, our initial topotecan plasma pharmacokinetic studies were designed to develop a pharmacokinetic limited sampling model for unbound topotecan that would minimize blood withdrawal and maximize information content. Therefore, using a variation of D-optimality (31, 32), we developed a limited sampling model with three samples based on the population variables (estimated via NONMEM) of unbound topotecan lactone that were determined in a group of mice.

In all subsequent microdialysis studies, we used this limited sampling strategy to collect plasma samples for topotecan pharmacokinetic studies. For each mouse, the topotecan plasma data were fit to a two-compartment model and clearance (CL_t), volumes (V_c, central compartment; V_p, peripheral compartment), and intercompartmental clearance (CL_p) were estimated along with their SE estimates. The individual mouse pharmacokinetics from plasma samples collected during microdialysis experiments were determined using maximum a posteriori probability (MAP) Bayesian estimation as implemented in ADAPT II (33). The prior variable distributions were determined from the above unbound topotecan lactone population pharmacokinetic studies we conducted. The area under the unbound topotecan lactone concentration-time curve (AUC) in plasma for each mouse was obtained by simulation.

Noncompartmental analysis of brain pharmacokinetic data. Topotecan carboxylate and lactone concentrations in brain ECF or ventricular CSF were corrected for the hydrolysis of topotecan lactone in pH 7.4 artificial CSF as defined previously (27). The AUC in brain ECF or ventricular CSF from time 0 to infinity was estimated using the linear trapezoidal method with the addition of a residual area as depicted in Eq. B

$$\text{AUC}_{\text{brain}}^{0\to\infty} = \sum_{i=1}^{n} \frac{C_i + C_{i-1}}{2} \times \Delta t + C_n/\beta \quad \text{(B)}$$

where C_i is the topotecan concentration in dialysate; Δt is the sample injection interval; Cn is the last measurable topotecan concentration; β is estimated by linear regression of the logarithm of the last four to five measurable concentrations.

The extent of CNS penetration of topotecan lactone was determined by the ratio of unbound topotecan lactone AUC in brain ECF or ventricular CSF to the unbound plasma topotecan lactone AUC. Student's *t* test was used to compare the unbound topotecan lactone brain to plasma AUC ratio after each treatment.

Compartmental analysis of brain pharmacokinetic data. A three-compartment model (34, 35) was developed to fit unbound topotecan lactone concentration-time data in brain parenchymal ECF or ventricular CSF and plasma as implemented in ADAPT II (Fig. 1). The variables describing topotecan disposition between the plasma and CSF or ECF (CL_{in}, CL_{out} and V_{ECF} or V_{CSF}) along with their SE estimates were estimated for each individual animal by fitting the model to the CSF or ECF data with the plasma pharmacokinetic variables (CL_t, V_c, CL_p, and V_p) fixed at the values obtained in the above described plasma pharmacokinetics section. To compare the noncompartmental and compartmental methods in

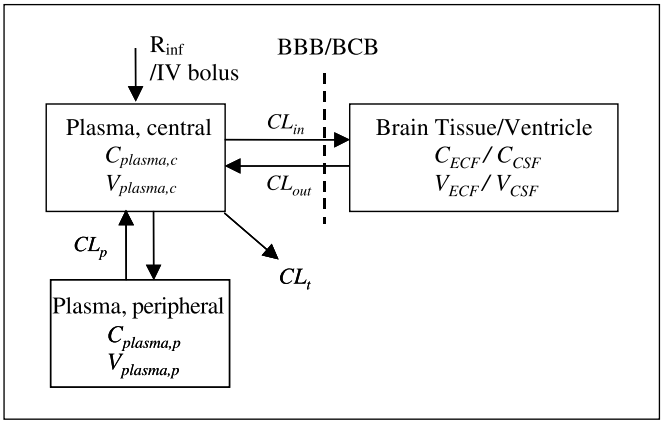

Figure 1. Pharmacokinetic model of unbound topotecan lactone in plasma and brain compartments. $V_{plasma,c}$ and $V_{plasma,p}$, volumes of distribution of unbound topotecan lactone in the central and peripheral plasma compartments (expressed as L/m^2); V_{ECF}/V_{CSF}, volume of distribution of unbound topotecan lactone in the respective brain tissue or ventricle (expressed as L/m^2); CL_t, systemic clearance of the drug from the central compartment (expressed as L/h/m^2); CL_p, intercompartmental clearance between central and peripheral plasma compartments (expressed as L/h/m^2); CL_{in} and CL_{out}, intercompartmental clearance between plasma and brain tissue or ventricle (expressed as L/h/m^2); R_{inf}, constant infusion rate (expressed as μg/h/m^2).

estimation of AUC in the brain, we calculated the ratio of CL_{in} to CL_{out}. Based on the relationship $CL_{in}/CL_{out} = AUC_{brain}/AUC_{plasma}$ (36), brain to plasma AUC ratios calculated from the noncompartmental and compartmental analyses were compared. Student's *t* test was used to compare the unbound topotecan lactone brain to plasma AUC ratio after each treatment.

Immunohistochemistry. Brains were collected from *Abcg2*$^{-/-}$ (Taconic, Germantown, NY) and wild-type FVB mice (The Jackson Laboratory). Tissues were fixed in 10% neutral buffered formalin overnight and embedded in paraffin before sectioning. The monoclonal antibody BXP-53 (1 μg/mL; Alexis Biochemicals, San Diego, CA) was used to detect Bcrp1 in mouse brain. Rat immunoglobulin G2a isotype was used as the negative control. The polyclonal goat anti-MDR antibody [5 μg/mL; MDR(C-19)K, Santa Cruz Biotechnology, Inc., Santa Cruz, CA] and nonimmunized goat immunoglobulin G were used for P-gp detection in mouse brain and the negative control, respectively.

Paraffin sections (3-5 μm) were stained using standard avidin-biotin complex immunohistochemical techniques. This consisted of streptavidin-horseradish peroxidase combined with an antigen retrieval step (DAKO Corp., Carpinteria, CA), and the addition of an avidin-biotin (Vector Labs, Burlingame, CA) blocking step before primary antibody application. Primary antibodies were incubated overnight at 4°C followed by secondary antibody, either biotinylated antirat or antigoat. Results were visualized with diaminobenzidine (DAKO), counterstained with hematoxylin (DAKO), and mounted in permanent medium (Fisher Scientific, Suwannee, GA).

Results

Topotecan protein binding. To assess the extent of topotecan protein binding and to determine if this protein binding differed among mouse strains, we measured topotecan plasma protein binding in multiple sources of murine plasma. We found that topotecan lactone protein binding in pooled murine plasma, C57/B6 plasma, and FVB plasma was 31.7 ± 3.8%, 32.3 ± 4.4%, and 36.4 ± 2.4%, respectively. Moreover, within the concentration range evaluated (50-5,000 ng/mL), no change in topotecan lactone protein binding was observed.

Gefitinib pharmacokinetic studies in mice. The typical gefitinib dosage used in published studies for mice is 100 mg/kg (18, 23). However, we wanted to use a gefitinib dosage that was

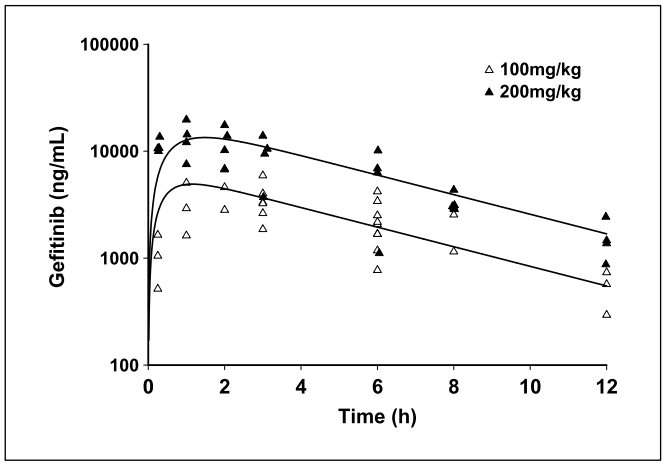

Figure 2. Gefitinib (ZD1839) plasma pharmacokinetics after 100 (△) and 200 (▲) mg/kg oral administration in FVB mice. Samples were extracted with *tert*-butyl ether with internal standard, separated on Phenomenex Synergy 4-μm MAX-RP C12 column (75 × 2.0 mm) with an isocratic mobile phase of acetonitrile/1.0% formic acid (30:70, v/v), and detected with a PE Sciex API 365 triple quadrupole MS using turbo ion spray source with positive ionization.

tolerable in mice, and that would maximize CNS gefitinib concentrations to modulate CNS transporters. Moreover, the timing of gefitinib administration to optimize modulation of CNS transporters was unknown. Thus, to gain insight into gefitinib disposition in FVB mice, we conducted a plasma gefitinib pharmacokinetic study of two gefitinib dosages (100 and 200 mg/kg). Mice tolerated both oral gefitinib dosages, and we found that it was absorbed quickly with the maximum gefitinib concentration achieved between 1 and 1.5 hours after oral administration (Fig. 2). Based on these results, we administered gefitinib orally 1 hour before topotecan administration at a dosage of 200 mg/kg.

Topotecan plasma pharmacokinetics studies in mice. Topotecan disposition in mice has been well studied; however, most studies used multiple numbers of mice at each time point with destructive sampling. Whereas, we desired to assess topotecan pharmacokinetics in the same mouse in which we did a microdialysis experiment. Thus, we developed a limited sampling model, which, in combination with MAP-Bayesian estimation, would allow us to estimate topotecan plasma pharmacokinetics in the individual mouse. We determined that the optimal sampling time points for the limited sampling model were 0.25, 1, and 3 hours after topotecan injection. For our MAP-Bayesian estimation, the prior variable distributions were estimated from our population pharmacokinetic study of six to eight mice. These values were clearance (CL_t) from the central compartment 54.6 ± 5.5 L/h/m^2, intercompartmental clearance (CL_p) 3.8 ± 0.5 L/h/m^2, and central and peripheral volumes of distribution (V_c and V_p) 26.3 ± 3.7 and 8.0 ± 1.4 L/m^2, respectively. The inter-animal variability for CL_t, CL_p, V_c, and V_p was 19.5%, 62.9%, 10.8%, and 38.7%, respectively. The prior variable distributions in the presence of gefitinib were clearance (CL_{tG}) from the central compartment, 25.9 ± 1.8 L/h/m^2; the intercompartmental clearance (CL_{pG}), 1.4 ± 0.4 L/h/m^2; and the central and peripheral volumes of distribution (V_{cG} and V_{pG}), 18.8 ± 2.4 and 2.1 ± 0.4 L/m^2, respectively. The inter-animal variability for CL_{tG}, CL_{pG}, V_{cG}, and V_{pG} was 17.0%, 12.3%, 25.7%, and 10.0%, respectively. Using MAP-Bayesian estimation and the above prior variable distributions, we estimated the unbound topotecan plasma pharmacokinetic variables for each individual mouse during each microdialysis experiment. For example, the individual variable estimates (CV%) for CL_t (L/hr/m^2) for the four microdialysis experiments presented in Fig. 4 were 29.8 (5.3), 46.7 (5.9), 25.2 (5.6), and 28.0 (5.6) for panels A to D, respectively, whereas the variable estimates (CV%) for V_c (L/m^2) were 21.9 (8.0), 24.4 (8.4), 22.1 (8.1), and 22.2 (8.1) for panels A to D, respectively.

Topotecan CNS penetration after 4 and 8 mg/kg. Using a microdialysis technique coupled with an online microbore HPLC system, we measured topotecan lactone concentrations in either brain ECF or ventricular CSF. As depicted in Fig. 3, the location of the probe track was verified either in the lateral ventricle or the parenchyma. The *in vivo* probe recoveries for topotecan in brain tissue ECF and ventricular CSF were 9.9 ± 3.5% and 7.9 ± 1.6%, respectively. Figure 4 shows representative unbound topotecan lactone concentration-time profiles for brain and plasma after 4 and 8 mg/kg topotecan injections. Unbound topotecan lactone concentrations in brain ECF were lower than those observed in plasma after 4 mg/kg topotecan injection (Fig. 4*A*), but when the topotecan dose was increased to 8 mg/kg, the unbound topotecan lactone in brain ECF reached the same level as that in the plasma in the elimination phase (Fig. 4*C*). On the other hand, the unbound topotecan lactone concentration in ventricular CSF was higher than that in plasma during the sampling time period for both the 4 mg/kg dose (Fig. 4*B*) and the 8 mg/kg dose (Fig. 4*D*).

To compare topotecan CNS penetration, we calculated an AUC ratio of unbound topotecan lactone in brain ECF or ventricular CSF to that in the plasma. As the topotecan dosage increased from 4 to 8 mg/kg, the brain ECF to plasma AUC ratio significantly increased (0.21 ± 0.04 and 0.61 ± 0.16; $P < 0.05$, Student's t test). Ventricular CSF to plasma AUC ratios were >1, but were not significantly different (1.18 ± 0.10 and 1.30 ± 0.13) after 4 and 8 mg/kg

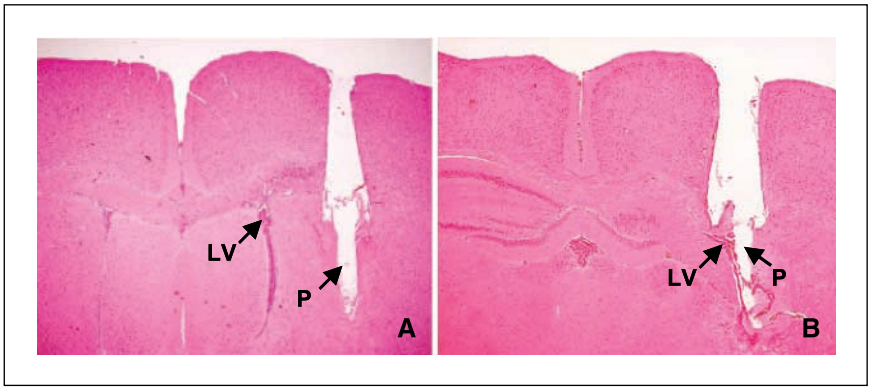

Figure 3. H&E staining of brain sections after probe insertion for microdialysis studies. *A,* microdialysis probe track (*P*) in the brain parenchyma (×20). *B,* microdialysis probe track in the lateral ventricle (*LV*; × 20). Both figures show no obvious bleeding after probe insertion.

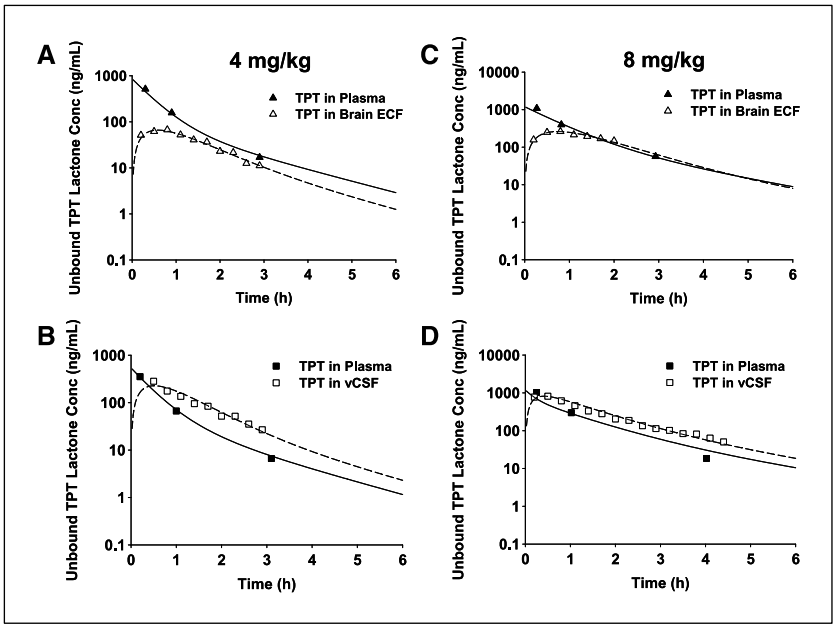

Figure 4. Representative unbound topotecan lactone concentration-time plots in plasma, brain parenchymal ECF, and ventricular CSF in FVB mice. *A* and *B,* unbound topotecan lactone in plasma (▲, ■) and brain parenchymal ECF (△) or ventricular CSF (*vCSF*; □) after 4 mg/kg topotecan i.v. injection. *C* and *D,* unbound topotecan lactone in plasma (▲, ■) and brain parenchymal ECF (△) or ventricular CSF (□) after 8 mg/kg topotecan i.v. injection. The fitted curves for plasma samples were simulated from the variables obtained using MAP-Bayesian estimation. The fitted curves for the brain pharmacokinetic data were obtained from a three-compartment model developed for the plasma and brain pharmacokinetic data using ADAPT II.

topotecan injections. The finding that the ventricular CSF to plasma AUC ratio was greater than unity strongly suggests an influx transport system at the blood-cerebrospinal fluid barrier.

Gefitinib enhanced topotecan penetration into brain ECF but decreased the penetration into the ventricular CSF. To address the objective of assessing the effect of a tyrosine kinase inhibitor on the brain parenchymal ECF and ventricular CSF penetration of topotecan, we studied the effect of gefitinib on topotecan CNS penetration. To avoid the potential for saturation of transporters at the blood-brain barrier seen with a higher topotecan dosage, a topotecan dosage of 4 mg/kg was used for these studies. The *in vivo* probe recoveries for topotecan lactone with gefitinib in brain tissue ECF and ventricular CSF were 7.7 ± 2.6% and 9.1 ± 1.9%, respectively. As shown in Fig. 5*A*, when mice were pretreated with 200 mg/kg gefitinib before 4 mg/kg topotecan, the unbound topotecan lactone concentrations in both plasma and brain ECF were elevated compared with that in controls (Fig. 4*A*), but the plasma concentrations were still higher than that in brain ECF. The unbound topotecan concentrations in ventricular CSF seemed to rapidly reach equilibrium with that in plasma in the presence of gefitinib (Fig. 5*B*).

In the presence of gefitinib, the unbound topotecan lactone brain ECF to plasma AUC ratio increased 1.6-fold to 0.35 ± 0.04 compared with control mice after 4 mg/kg topotecan (Fig. 5*C, left*; $P < 0.05$, Student's *t* test) indicating that gefitinib enhanced ECF penetration. On the other hand, gefitinib decreased the

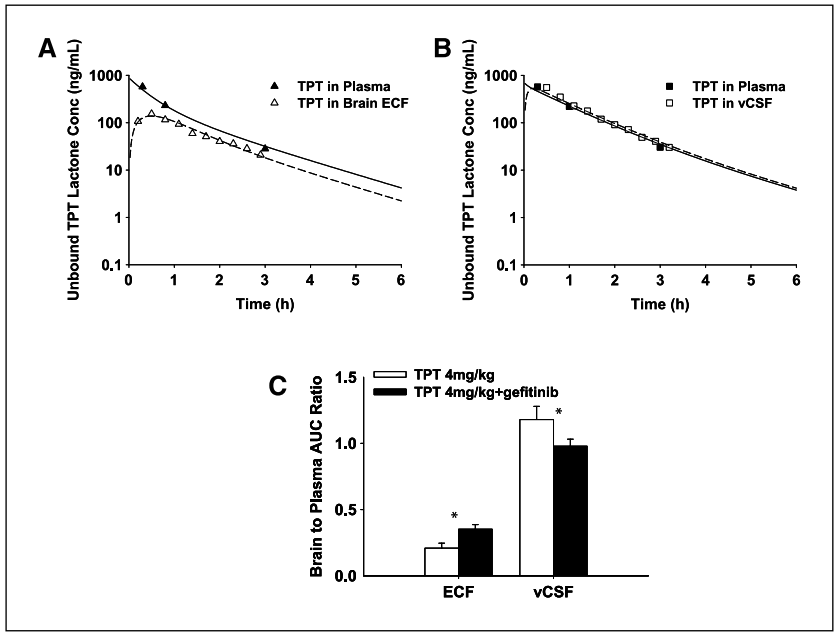

Figure 5. Representative unbound topotecan lactone concentration-time plots in plasma, brain parenchymal ECF, and ventricular CSF in FVB mice pretreated with 200 mg/kg gefitinib. Unbound topotecan lactone in plasma (▲, ■) and brain parenchymal ECF (*A*; △) or ventricular CSF (*B*; □) after 4 mg/kg topotecan i.v. injection. *C,* brain to plasma AUC ratio of unbound topotecan lactone after 4 mg/kg topotecan i.v. injection with and without gefitinib. *, $P < 0.05$ (Student's *t* test).

Table 1. A comparison of brain to plasma AUC ratio of unbound topotecan lactone using noncompartmental and compartmental analyses

	CL_{in} ($L/h/m^2$)	CL_{out} ($L/h/m^2$)	CL_{in}/CL_{out} (compartmental)	AUC ratio (noncompartmental)
Topotecan at blood-brain barrier	2.10 (1.11)*	10.73 (7.32)	0.21 (0.06)	0.21 (0.04)
Topotecan + gefitinib at blood-brain barrier	1.78 (1.81)	6.03 (4.35)	0.33 (0.07)	0.35 (0.03)
Topotecan at blood-cerebrospinal fluid barrier	3.92 (0.41)	3.08 (0.31)	1.29 (0.26)	1.18 (0.06)
Topotecan + gefitinib at blood-cerebrospinal fluid barrier	25.36 (6.87)	26.16 (4.16)	0.96 (0.14)	0.98 (0.05)

*Mean (SD); n = 3 or 4.

ventricular CSF to plasma AUC ratio to 0.98 ± 0.05 compared with control mice (Fig. 5*C, right*; $P < 0.05$, Student's t test). This decrease in ventricular CSF topotecan AUC ratio suggests that gefitinib has inhibited influx at the blood-cerebrospinal fluid barrier.

Besides calculating the topotecan AUC in brain using noncompartmental methods, we also developed a three-compartment model to estimate intercompartmental clearance between the brain and the plasma (CL_{in} and CL_{out}). The pharmacokinetic variables for unbound plasma topotecan lactone for each individual animal were obtained from MAP-Bayesian approach and fixed in the compartmental analysis. Examples of fitted curves are shown in Figs. 4 and 5. Presented in Table 1 are the mean (±SD; n = 3 or 4) compartmental variable estimates (i.e., CL_{in} and CL_{out}) and derived ratios (e.g., CL_{in}/CL_{out}). Treatment with the tyrosine kinase inhibitor gefitinib did not alter the influx clearance (CL_{in}) at the blood-brain barrier. This is compared with the mean efflux clearance (CL_{out}) at the blood-brain barrier, which decreased 44% in the presence of gefitinib, suggesting inhibition of efflux transport. CL_{in} and CL_{out} both were observed to increase at the blood-cerebrospinal fluid barrier with administration of gefitinib. Based on the relationship $CL_{in}/CL_{out} = AUC_{brain}/AUC_{plasma}$ (36), the ratio of CL_{in} to CL_{out} is the same as the brain to plasma AUC ratio. A comparison of the brain to plasma AUC ratio obtained from compartmental and noncompartmental analyses showed similar results, as presented in Table 1.

Localization of BCRP and P-gp. Compared with the blood-brain barrier, expression of ABC transporters at the blood-cerebrospinal fluid barrier has not been extensively studied. Only P-gp, MRP4, and MRP1 have been reported at the choroid plexus (14, 37). Our pharmacokinetic results suggest the presence of an influx system for topotecan at the choroid plexus. Thus, we examined the expression of Bcrp1 and P-gp at the choroid plexus by immunohistochemistry. We did immunohistochemistry on fixed whole brains that were serially cross-sectioned and embedded in paraffin blocks. Immunohistochemistry was done on specimens from both wild-type and *Abcg2*$^{-/-}$ mice. Bcrp1 was detected at the apical aspect of the choroid plexus in wild-type mice (Fig. 6*A*), but was absent in the *Abcg2*$^{-/-}$ mice (Fig. 6*C*). P-gp expression was also detected in mouse choroid plexus (Fig. 7*A*) and showed a granular staining pattern throughout the cytoplasm, similar to what was reported by Rao et al. (37) in rat and human and by Warren et al. (38) in nonhuman primates.

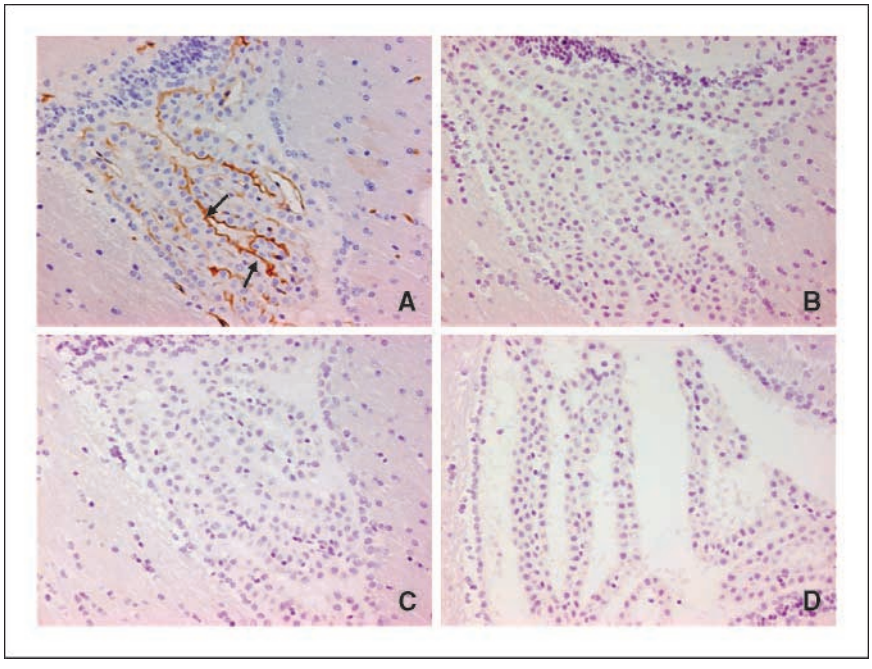

Figure 6. Immunohistochemical staining of Bcrp1 at choroid plexus. Bcrp1 was detected at the apical side of choroid plexus in wild-type mouse (*A, arrows*; × 200), but was absent in the *Abcg2*$^{-/-}$ mice (*C*; × 200). Negative controls showed no Bcrp1 staining in wild-type mouse (*B*; × 200) and *Abcg2*$^{-/-}$ mice (*D*; × 200).

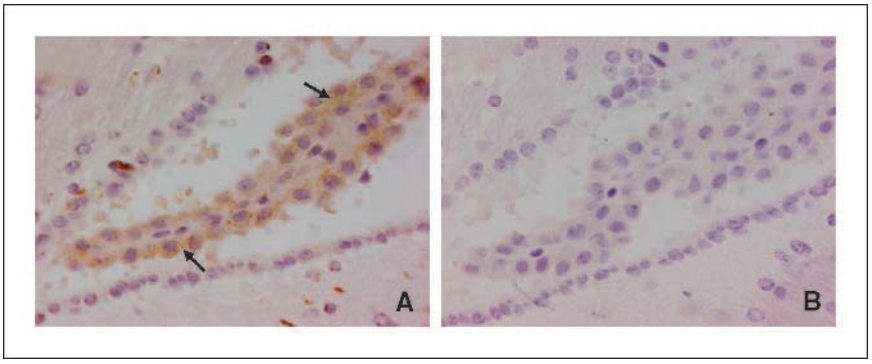

Figure 7. Immunohistochemical staining of P-gp at choroid plexus. P-gp expression was detected in mouse choroid plexus and showed a granular staining pattern throughout the cytoplasm (*A*; × 400) but not in the negative control (*B*; × 400).

Discussion

We determined the brain ECF (i.e., blood-brain barrier) and ventricular CSF (i.e., blood-cerebrospinal fluid barrier) penetration of topotecan lactone in mice and showed that topotecan concentrations in brain ECF were less than those in plasma at 4 mg/kg topotecan dose. This was in contrast with the topotecan concentrations in the ventricular CSF, which were greater than plasma concentrations at both 4 and 8 mg/kg topotecan dosages. When mice were pretreated with the tyrosine kinase inhibitor gefitinib, we found that the topotecan brain ECF to plasma ratio was increased by 1.6-fold, whereas, surprisingly, the topotecan ventricular CSF to plasma ratio was decreased. Finally, we found that Bcrp1 was expressed on the apical aspect of the choroid plexus of FVB mice, which, coupled with the orientation of transporters expressed at the blood-brain barrier (39), would explain the differential effect of the tyrosine kinase inhibitor modulator on topotecan brain penetration.

We used microdialysis sampling, coupled with online microbore HPLC, to measure topotecan concentrations in parenchymal ECF and ventricular CSF of mice. Microdialysis experiments in mice are exceedingly difficult for several reasons. One limitation, the small dialysate sample volume available for analysis, was overcome by use of online injections and a sensitive fluorescence detector. Although probe recoveries were low, they were stable and adequate to measure topotecan concentrations for the duration of our experiments. The actual implantation of a microdialysis cannula and probe is an invasive process. Thus, it is critical to allow for adequate recovery afterwards so that acute tissue reaction can be minimized. In our studies, we have allowed 3 to 5 days for the animal to recover from the cannula implantation and a 60-minute stabilization period after probe insertion based on the logistics of our study. Recognizing the 60-minute time frame was empirical and may have potential to contribute to variability in our results, we chose to use several methodologic approaches to address this potential problem. First, we made sure that the equilibration period was consistent among animals, which would enhance our ability to compare data among experiments. Second, we used the smallest microdialysis probe available for our experiments (probe outer diameter, 0.22 mm; 1-mm membrane), inserting it very slowly into the tissue to minimize the damage. Finally, to confirm that minimal tissue damage had occurred and that the blood-brain barrier or blood-cerebrospinal fluid barrier integrity was intact, after each experiment we removed the mouse brain and evaluated the extent of bleeding caused by probe implantation. Data from animals that had obvious bleeding into the tissue would be excluded from analysis.

To assess the extent of topotecan brain penetration, we used an AUC ratio of unbound drug in the brain compartments to that in plasma. To calculate the unbound drug AUC in brain, we used a different equation from other published methods because of the unique online microbore HPLC system used in our study. With the microbore HPLC system, we collected the dialysate into a 2-μL sample loop, which allows for overfilling of the loop by ~4-fold based on the preset flow rate (0.5 μL/min) and sample loading interval (15 minutes). Thus, we made the assumption that the drug concentration in the sample loop at the time of each injection was not the integrated concentration over the collection time interval, but was the drug concentration at the time point when it was injected. With our online injection system, the samples were run in "real-time," permitting the use of the equation we proposed to calculate the AUC in the brain ECF and ventricular CSF. Furthermore, we obtained unbound drug concentration to calculate AUC in plasma because that was the form that can freely diffuse or be transported across the blood-brain and blood-cerebrospinal fluid barriers and was considered the pharmacologically active form (i.e., available for metabolism or transport). The AUC ratio has significant advantages when compared with a ratio calculated from a single time point. These include not being influenced by the time a sample was obtained relative to the time the dose was administered, more flexibility in sample timing, and less bias in calculating brain penetration. The results of the unbound topotecan AUC ratio allowed us to distinguish the potential mechanism of drug transport at the blood-brain and blood-cerebrospinal fluid barriers. In our study, the AUC ratio of unbound topotecan in brain parenchymal ECF to plasma was 0.21 ± 0.04 at a topotecan dosage of 4 mg/kg. This was much less than unity, which suggested active efflux transport activity at the blood-brain barrier. We were not surprised at this finding because the known ABC transporters expressed at the blood-brain barrier are located at the apical side (e.g., BCRP, P-gp, MRP4), and would thus pump substrates out of the brain back to the blood. Moreover, topotecan is a known substrate for these transporters (12, 14, 16). When we doubled the topotecan dosage, the AUC ratio increased ~3-fold, suggesting the possibility of partial saturation. Because we observed an AUC ratio of unbound topotecan in ventricular CSF to plasma ratio greater than unity at both topotecan dosages, this strongly suggests the presence of an influx transport system at the blood-cerebrospinal fluid barrier.

Our findings have potential clinical relevance for the therapy of patients with primary CNS tumors. The most common type of primary CNS tumor in adults is glioblastoma multiforme, which is a parenchymal-based tumor (i.e., ECF, blood-brain barrier), whereas in children, it is more common to find primary CNS tumors that

are neuroaxis based (i.e., CSF, blood-cerebrospinal fluid barrier). We observed that topotecan penetration into the parenchymal ECF was much less than penetration into the ventricular CSF. Thus, it could be expected that even if topotecan were an active drug *in vitro* against glial tumors, it would be unlikely to have *in vivo* or clinical activity in this tumor model. However, topotecan does have avid CSF penetration and has been shown to have significant antitumor activity in children with high-risk medulloblastoma (5). Our results emphasize the point that "CNS penetration" for a drug cannot simply be extrapolated from a measurement of CSF drug penetration.

To assess the effect of a tyrosine kinase inhibitor on topotecan penetration into brain, we used the 4-anilinoquinazoline gefitinib on a schedule and dosage that was based on our preclinical studies that would optimize modulation of ABC transporters. In the presence of gefitinib, the topotecan ECF penetration increased, suggesting that gefitinib blocked the efflux transporters. On the other hand, gefitinib decreased the ventricular CSF to plasma AUC ratio, indicating inhibition of the influx transport system at the blood-cerebrospinal fluid barrier. Although we used topotecan as our probe drug and gefitinib as the transporter modulator, it is likely that this model could be used to assess the effect of penetration by other transporter modulators. It further emphasizes the point raised above that when drugs are used in combination (e.g., topotecan and tyrosine kinase inhibitors), CNS drug penetration cannot necessarily be determined by measuring the easily accessible surrogate of CSF drug concentrations. Rather, differences may exist in ECF penetration as compared with CSF penetration depending on the specificity and orientation of transporters.

We report for the first time the expression of Bcrp1 at the apical aspect of the mouse and rat choroid plexus (data not shown). The expression of Bcrp1 is focused at the border of the apical aspect of choroid plexus, which indicates drug transport direction towards the CSF. Because topotecan is an excellent BCRP substrate, the orientation of Bcrp1 may facilitate topotecan transport into CSF, which results in high topotecan ventricular CSF penetration. Besides Bcrp1, we also detected P-gp expression in mouse choroid plexus. Unlike Bcrp1, the immunohistochemical staining pattern of P-gp in choroid plexus seemed to be more uniformly scattered and granular throughout the cytoplasm versus being discretely localized to the border of epithelial cells. The granular pattern noted in our samples has previously been observed in the choroid plexus of rat, nonhuman primates, and human (37, 38). It is commonly recognized that P-gp has a predominantly subapical distribution in choroid plexus epithelia (37, 39). In this case, P-gp may also play a role in transporting topotecan into the CSF.

In conclusion, topotecan brain ECF penetration was much lower compared with ventricular CSF penetration. Gefitinib increased topotecan brain ECF penetration but decreased ventricular CSF penetration. These results are consistent with the possibility that expression of Bcrp1 and P-gp at the apical side of the choroid plexus facilitates an influx transport mechanism across the blood-cerebrospinal fluid barrier, resulting in high topotecan CSF penetration, which could be inhibited by tyrosine kinase inhibitors like gefitinib. To determine if this is clinically relevant, it will be necessary to examine whether BCRP is also expressed at the apical side of the human choroid plexus. Our results also suggest the possible use of tyrosine kinase inhibitors to enhance brain parenchymal ECF penetration of selected anticancer drugs in the clinic. However, caution must be taken in combining tyrosine kinase inhibitors with anticancer drugs because this may not necessarily enhance the CSF drug penetration for drugs that are substrates for influx transporters.

Acknowledgments

Received 3/15/2006; revised 8/23/2006; accepted 9/29/2006.

Grant support: Public Health Service awards NIH grants GM071321, CA21765 (Cancer Center Support Grant), and CA23099, and the American Lebanese Syrian Associated Charities.

The costs of publication of this article were defrayed in part by the payment of page charges. This article must therefore be hereby marked *advertisement* in accordance with 18 U.S.C. Section 1734 solely to indicate this fact.

References

1. Hsiang YH, Liu LF. Identification of mammalian DNA topoisomerase I as an intracellular target of the anticancer drug camptothecin. Cancer Res 1988;48:1722–6.
2. Hsiang YH, Hertzberg R, Hecht S, Liu LF. Camptothecin induces protein-linked DNA breaks via mammalian DNA topoisomerase I. J Biol Chem 1985;260:14873–8.
3. Pawlik CA, Houghton PJ, Stewart CF, et al. Effective schedules of exposure of medulloblastoma and rhabdomyosarcoma xenografts to topotecan correlate with *in vitro* assays. Clin Cancer Res 1998;4:1995–2002.
4. Friedman HS, Houghton PJ, Schold SC, Keir S, Bigner DD. Activity of 9-dimethylaminomethyl-10-hydroxycamptothecin against pediatric and adult central nervous system tumor xenografts. Cancer Chemother Pharmacol 1994;34:171–4.
5. Stewart CF, Iacono LC, Chintagumpala M, et al. Results of a phase II upfront window of pharmacokinetically guided topotecan in high-risk medulloblastoma and supratentorial primitive neuroectodermal tumor. J Clin Oncol 2004;22:3357–65.
6. Bernier-Chastagner V, Grill J, Doz F, et al. Topotecan as a radiosensitizer in the treatment of children with malignant diffuse brainstem gliomas: results of a French Society of Paediatric Oncology Phase II Study. Cancer 2005;104:2792–7.
7. Chintagumpala MM, Friedman HS, Stewart CF, et al. A phase II window trial of procarbazine and topotecan in children with high-grade glioma: a report from the children's oncology group. J Neurooncol 2006;77:193–8.
8. Blaney SM, Phillips PC, Packer RJ, et al. Phase II evaluation of topotecan for pediatric central nervous system tumors. Cancer 1996;78:527–31.
9. Loscher W, Potschka H. Drug resistance in brain diseases and the role of drug efflux transporters. Nat Rev Neurosci 2005;6:591–602.
10. Castro MG, Cowen R, Williamson IK, et al. Current and future strategies for the treatment of malignant brain tumors. Pharmacol Ther 2003;98:71–108.
11. Pardridge WM. Log(BB), PS products and in silico models of drug brain penetration. Drug Discov Today 2004;9:392–3.
12. Hendricks CB, Rowinsky EK, Grochow LB, Donehower RC, Kaufmann SH. Effect of P-glycoprotein expression on the accumulation and cytotoxicity of topotecan (SK&F 104864), a new camptothecin analogue. Cancer Res 1992;52:2268–78.
13. Chen AY, Yu C, Potmesil M, et al. Camptothecin overcomes MDR1-mediated resistance in human KB carcinoma cells. Cancer Res 1991;51:6039–44.
14. Leggas M, Adachi M, Scheffer GL, et al. Mrp4 confers resistance to topotecan and protects the brain from chemotherapy. Mol Cell Biol 2004;24:7612–21.
15. Maliepaard M, van Gastelen MA, Tohgo A, et al. Circumvention of breast cancer resistance protein (BCRP)-mediated resistance to camptothecins *in vitro* using non-substrate drugs or the BCRP inhibitor GF120918. Clin Cancer Res 2001;7:935–41.
16. Maliepaard M, van Gastelen MA, de Jong LA, et al. Overexpression of the BCRP/MXR/ABCP gene in a topotecan-selected ovarian tumor cell line. Cancer Res 1999;59:4559–63.
17. Kruijtzer CM, Beijnen JH, Rosing H, et al. Increased oral bioavailability of topotecan in combination with the breast cancer resistance protein and P-glycoprotein inhibitor GF120918. J Clin Oncol 2002;20:2943–50.
18. Leggas M, Panetta JC, Zhuang Y, et al. *In vivo* inhibition of multiple ABC transporters by an oral tyrosine kinase inhibitor. Cancer Res 2006;66:4802–7.
19. Kitazaki T, Oka M, Nakamura Y, et al. Gefitinib, an EGFR tyrosine kinase inhibitor, directly inhibits the function of P-glycoprotein in multidrug resistant cancer cells. Lung Cancer 2005;49:337–43.
20. Nakamura Y, Oka M, Soda H, et al. Gefitinib ("Iressa", ZD1839), an epidermal growth factor receptor tyrosine kinase inhibitor, reverses breast cancer resistance protein/ABCG2-mediated drug resistance. Cancer Res 2005;65:1541–6.
21. Yang CH, Huang CJ, Yang CS, et al. Gefitinib reverses chemotherapy resistance in gefitinib-insensitive multidrug resistant cancer cells expressing ATP-binding cassette family protein. Cancer Res 2005;65:6943–9.
22. Erlichman C, Boerner SA, Hallgren CG, et al. The HER tyrosine kinase inhibitor CI1033 enhances cytotoxicity of 7-ethyl-10-hydroxycamptothecin and topotecan by inhibiting breast cancer resistance protein-mediated drug efflux. Cancer Res 2001;61:739–48.

23. Stewart CF, Leggas M, Schuetz JD, et al. Gefitinib enhances the antitumor activity and oral bioavailability of irinotecan in mice. Cancer Res 2004;64:7491–9.
24. Baker SD, Heideman RL, Crom WR, et al. Cerebrospinal fluid pharmacokinetics and penetration of continuous infusion topotecan in children with central nervous system tumors. Cancer Chemother Pharmacol 1996;37:195–202.
25. Furman WL, Baker SD, Pratt CB, et al. Escalating systemic exposure of continuous infusion topotecan in children with recurrent acute leukemia. J Clin Oncol 1996;14:1504–11.
26. Bai F, Iacono LC, Johnston B, Stewart CF. Determination of gefitinib in plasma by liquid chromatography with a C_{12} column and electrospray tandem mass spectrometry detection. J Liq Chromatogr Relat Tech 2004;27:2743–58.
27. Leggas M, Zhuang Y, Welden J, et al. Microbore HPLC method with online microdialysis for measurement of topotecan lactone and carboxylate in murine CSF. J Pharm Sci 2004;93:2284–95.
28. Elmquist WF, Sawchuk RJ. Application of microdialysis in pharmacokinetic studies. Pharm Res 1997;14:267–88.
29. Le Quellec A, Dupin S, Genissel P, et al. Microdialysis probes calibration: gradient and tissue dependent changes in no net flux and reverse dialysis methods. J Pharmacol Toxicol Methods 1995;33:11–6.
30. Beal SL, Sheiner LB. NONMEM users' guide. GloboMax LLC; 1992.
31. D'Argenio DZ. Optimal sampling times for pharmacokinetic experiments. J Pharmacokinet Biopharm 1981;9:739–56.
32. Panetta JC, Iacono LC, Adamson PC, Stewart CF. The importance of pharmacokinetic limited sampling models for childhood cancer drug development. Clin Cancer Res 2003;9:5068–77.
33. D'Argenio DZ, Schumitzky A. ADAPT II user's guide: pharmacokinetic/pharmacodynamic systems analysis software. Biomedical Simulations Resource; 1997.
34. Hammarlund-Udenaes M, Paalzow LK, de Lange EC. Drug equilibration across the blood-brain barrier-pharmacokinetic considerations based on the microdialysis method. Pharm Res 1997;14:128–34.
35. Gupta A, Chatelain P, Massingham R, Jonsson EN, Hammarlund-Udenaes M. Brain distribution of cetirizine enantiomers: comparison of three different tissue-to-plasma partition coefficients: K(p), K(p,u), and K(p,uu). Drug Metab Dispos 2006;34:318–23.
36. Wong SL, Van BK, Sawchuk RJ. Distributional transport kinetics of zidovudine between plasma and brain extracellular fluid/cerebrospinal fluid in the rabbit: investigation of the inhibitory effect of probenecid utilizing microdialysis. J Pharmacol Exp Ther 1993;264:899–909.
37. Rao VV, Dahlheimer JL, Bardgett ME, et al. Choroid plexus epithelial expression of MDR1 P glycoprotein and multidrug resistance-associated protein contribute to the blood-cerebrospinal-fluid drug-permeability barrier. Proc Natl Acad Sci U S A 1999;96:3900–5.
38. Warren KE, Patel MC, McCully CM, Montuenga LM, Balis FM. Effect of P-glycoprotein modulation with cyclosporin A on cerebrospinal fluid penetration of doxorubicin in non-human primates. Cancer Chemother Pharmacol 2000;45:207–12.
39. Szakacs G, Paterson JK, Ludwig JA, Booth-Genthe C, Gottesman MM. Targeting multidrug resistance in cancer. Nat Rev Drug Discov 2006;5:219–34.